SCIENCE CHINA
Technological Sciences

·Special Topic · Characteristics, Dynamics and Control in Neuronal Disease Systems
• Article •

July 2017 Vol.60 No.7: 974–984
doi: 10.1007/s11431-016-9045-4

Seizures dynamics in a neural field model of cortical-thalamic circuitry

ZHANG HongHui[1*], ZHENG YanHong[2], SU JianZhong[3] & XIAO PengCheng[4]

[1] *School of Natural and Applied Science, Northwestern Polytechnical University, Shaanxi 710012, China;*
[2] *College of Mathematics and Computer Science, Fujian Normal University, Fuzhou 350007, China;*
[3] *Department of Mathematics, the University of Texas at Arlington, Texas 76019, USA;*
[4] *Department of Mathematics, University of Evansville, Indiana 47722, USA*

Received December 15, 2016; accepted March 27, 2017; published online June 21, 2017

The focus of this study is to explore the mechanisms during seizure behavior using a physiologically motivated by corticothalamic circuity. The model is based on the assumption that, the inhibitory projects from thalamus reticular nucleus (TRN) to specific relay nuclei (SRN) are mediated by $GABA_A$ and $GABA_B$ receptors which react different time scales in synaptic transmission. Secondly, we include the effects of slow modulation on the threshold current of TRN population that were found to generate bursting behavior. Our model can reproduce healthy and pathological dynamics including wake, spindle, deep sleep, and also seizure states. In addition, contour maps are used to explore the transition of different activity states. It is worthy to point out seizure duration is significantly affected by a time-varying delay as illustrated in our numerical simulation. Finally, a reduced model ignoring the cerebral cortex mass can also capture the feature of spike wave discharge as generated in the full network.

seizure, spike wave, neural field, modeling, corticothalamic

Citation: Zhang H H, Zheng Y H, Su J Z, et al. Seizures dynamics in a neural field model of cortical-thalamic circuitry. Sci China Tech Sci, 2017, 60: 974–984, doi: 10.1007/s11431-016-9045-4

1 Introduction

Epilepsy is one of the most common neurological disorders characterized by recurrent seizures which affects up to 1%–5% of people all over world as reported [1]. The recurrent seizures are synchronized, paroxysmal, and excessive discharges of neural populations, and they are classified into two main categories: partial and generalized [2]. In essence, a partial seizure can remain confined to its focus, or can migrate to other brain areas, causing a secondary generalized seizure. Therefore, seizures are generated by synchronized bursting of a group of cortical neurons, leading to increased coherence in the recorded signal. Generalized seizures are pathological brain rhythms across most or all of the cortical regions and are associated with loss of cognitive activity, while absence and tonic-clonic seizures are two common generalized seizures in human. In clinical, these transient seizure events can be observed by the electroencephalogram (EEG) [3]. Electrode probes measure the mean local field potential generated by synchronous activity of large assemblies of pyramidal cells as well as excitatory and inhibitory interneurons located in the vicinity of the probe contact [4].

The cause of epilepsy and its effects on cerebral functions is so complex that it is a formidable task to conceive a single framework to characterize all the pathophysiological changes in epilepsy at molecular, cellular and neuronal network level [5]. Considering seizures can be viewed as a time involving or dynamical disease [6,7], mathematical modeling can be

*Corresponding author (email: haozhucy@nwpu.edu.cn)

conducted to obtain new insights into epileptic seizures [8–11]. Indeed they have been successfully used to gain in-depth knowledge and generate novel hypotheses related to the cellular and network level brain mechanisms of epileptic seizure, and as a tool to guide the prediction of impending seizure and alternative therapeutic treatment [12,13].

Neural mass models initiated by Freeman [14,15] and then used in mathematical models are so successful in modeling [16–18] and produce brain rhythm observed in macroscopic measurements such as EEG [19–22]. It is known that the thalamus and cortical interactions are found to play an essential role in the generation of epilepsy spike-wave discharge [23,24] as a classical symptom of absence seizure [25–27]. Therefore a macro scale model using neural field theory based on corticothalamic system has been often used and modified and enhanced in seizure [28–31]. This class of neural field model describes the dynamical behaviors of large interacting groups of neurons in cortex and thalamus, which are referred as two neural layers [32–34]. Thalamic component is assumed to consist of two neural masses, an excitatory mass of SRN and a inhibitory mass of TRN. Similarly, the cortical component incorporates both a mass of excitatory pyramidal cell and inhibitory interneurons.

Here we study the seizure behavior through enhancing Freeman's corticothalamic neural field model, which describes the relevant brain activity through a second order delay differential equation. Our model has been able to reproduce many properties of EEG observation in a physiologically plausible parameter region.

2 Methods

The cortico-thalamic circuity studied here is a mean field neural model since the variables represent the local mean value of a physiological process [35,36]. It is based on several dynamical variables within three masses: a mass of cortical pyramidal neurons, cells in SRN and cells in TRN as illustrated schematically in Figure 1.

Combining some realistic assumptions extracted from theoretical studies and experimental clinical data [37–39], especially crucial works in refs. [40,41] which enable the partial differential equation (PDE) description of the cortical propagation and a reduction to an ordinary differential equation (ODE) model, our model can be described by a system of delay differential equations:

$$\frac{\mathrm{d}\dot{V}_e}{\mathrm{d}t} = \alpha\beta\left[v_{ee}\varphi_e + v_{ei}S_e(V_e) + v_{es}S_s(V_s) - \left(\frac{1}{\alpha}+\frac{1}{\beta}\right)\dot{V}_e - V_e\right],$$

$$\frac{\mathrm{d}\dot{V}_r}{\mathrm{d}t} = \alpha\beta\left[v_{re}\varphi_e + v_{rs}S_s(V_s) - \left(\frac{1}{\alpha}+\frac{1}{\beta}\right)\dot{V}_r - V_r\right],$$

$$\frac{\mathrm{d}\dot{V}_s}{\mathrm{d}t} = \alpha\beta[v_{se}\varphi_e + v_{sr}S_{ra}(V_r) + v_{sr}S_{rb}(V_r(t-\tau))$$

$$- v_{sn}\varphi_n - \left(\frac{1}{\alpha}+\frac{1}{\beta}\right)\dot{V}_s - V_s],$$

$$\frac{\mathrm{d}\dot{\varphi}_e}{\mathrm{d}t} = \gamma_e^2\left[S_e(V_e) - \frac{2}{\gamma}\dot{\varphi}_e - \varphi_e\right],$$

$$\frac{\mathrm{d}X}{\mathrm{d}t} = -\frac{1}{\tau_X}(X - X_\infty),$$

$$\frac{\mathrm{d}H}{\mathrm{d}t} = -\frac{1}{\tau_H}(H - 3X),$$

where

$$\frac{\mathrm{d}V_e}{\mathrm{d}t} = \dot{V}_e, \quad \frac{\mathrm{d}V_r}{\mathrm{d}t} = \dot{V}_r, \quad \frac{\mathrm{d}V_s}{\mathrm{d}t} = \dot{V}_s, \quad \frac{\mathrm{d}\varphi_e}{\mathrm{d}t} = \dot{\varphi}_e,$$

$$S_{e,s}(v) = S_{ra}(v)\frac{Q_{\max}}{1+\mathrm{e}^{(-\frac{v-\theta}{\sigma})}}, \quad S_{rb}(v) = \frac{Q_{\max-r}}{1+\mathrm{e}^{(-\frac{v-\theta_r}{\sigma})}},$$

$$\theta_r = \frac{I_c - 3I_b X + (I_b - I_a)H}{\mu},$$

$$I_a = I_b - g_H(V_{\mathrm{eff}} - V_K),$$

$$I_b = \frac{g_X(V_{\mathrm{eff}} - V_K)}{3}.$$

Each of the neural mass (cortex, TRN, SRN) is described by its average membrane potential $V_{e,r,s}$, while cortical neurons are described by the sequence firing ratio $\phi_{e,r,s}$ to take into account long range connections among cortical cells, and external inputs into SRN are represented by ϕ_n. The parameter $v_{ab}(i,e,r,s,n)$ denotes the weighting of inputs via synapse from population b onto population a.

In addition, the X-H system is slow currents modulating the bursting behavior in TRN via changes to the firing rate. Sigmoid function S, S_r is a good approximation for the firing

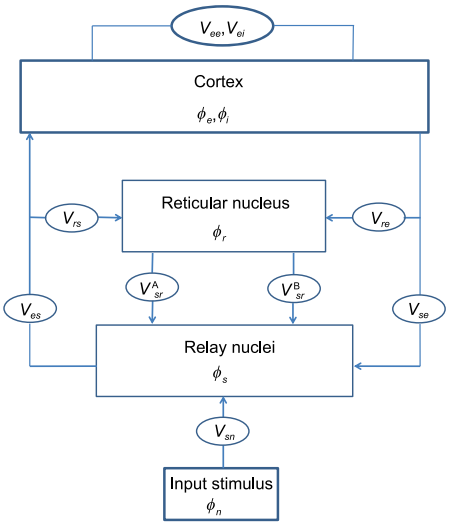

Figure 1 (Color online) Schematics diagram of principle neural fields and loops within the corticothalamic model, representing three neural masses as the main components of the thalamocortical dynamics. The lines represent connections between different masses, the mass response are ϕ_e (excitatory and inhibitory), ϕ_r (inhibitory) and ϕ_s (excitatory), while ϕ_n represents subcortical input, including a noise component.

rate produced by the voltage at each population $V_{e,r,s}$, which generates outgoing activity propagated to other population [42]. $Q_{\max}$ is the maximal firing rate at which the sigmoid firing function saturates, the threshold voltage θ is relative to the threshold current I_θ and the conductance per unite area μ. The *X-H* system acts as a feedback system due to the following principle: when the firing rate of SRN is high, it shifts the sigmoid to the right, and when the firing rate of SRN is low, the sigmoid is shifted to the left. This mechanism is a key point to modulate bursting between seizure episodes. More explanation and default values can be found in refs. [43,44].

The post synaptic membrane conductance of SRN neurons for both AMPA (excitatory) and GABA (inhibitory) from the TRN cell population is responsible for sustaining and modulating the firing activity. Particularly, inhibition in TRN neurons has been found to be a crucial component in the development of spike wave activity, and thus we focus our attention on modeling two important receptors ligand-gated $GABA_A$ and the secondary messenger-gated $GABA_B$ [37]. Moreover, $GABA_B$ mediated synapses, unlike $GABA_A$ synapses, activate G-proteins which in turn act as the secondary messengers and initiate the opening of ion channels. The inhibitory post-synaptic potential mediated by $GABA_B$ receptors has a much slower time scale than those mediated by $GABA_A$, then we expect if TRN neurons fires, the $GABA_B$ mediating connection to the SRN will be delayed compared to others or not. Hence, we incorporate a time delayed connection from TRN to SRN populations in our model.

3 Simulation results

As we know, the mean field models have been used to describe the brain mass activity recorded by EEG signals and then try to explore the mechanism from normal states to pathology states. Since EEG detection is operated in the cortex layer and is a summation of activity from a group of neuron scalp within the adjacent region, so we assume a functional relationship between cerebral cortex variable ϕ_e and the scalp EEG voltage. Accordingly, we mainly focus on ϕ_e as an approximation of EEG signals.

3.1 EEG pattern

Essentially, our proposed model can reproduce normal states and also seizure states as other corticothalamic neural field models have already realized. Under different excitatory and inhibitory synapses, activity of each cell population in cortex-thalamus circuit undergoes significant changes. In our model simulation, varying connection strength between each population, such as v_{se}, v_{rs}, and firing ratio of cortex denoted by ϕ_e behaves differently, including normal states and also seizure states.

The comparison of different brain states wake, spindle, sleep, seizure, produced by our model can be outlined in Figure 2. We can have a simple and brief explanation: in normal state, the firing rate is lower as shown in Figure 2(a), (c) and (e) while in seizure state the firing state is much higher as shown in Figure 2(g). More specially, wake state has the lowest firing ratio of cortex denoted by ϕ_e lower than 5 Hz, while spindle state and deep sleep state are around 7–9 Hz. This implies that magnitude of firing rate is one distinguishing feature among different states.

Another remarkable characteristics is demonstrated by Figure 2(b), (d), (f) and (h), in which the frequency of firing ratio in seizure state alternating with obvious oscillation and other normal states seems to smoothly decrease in the spectrogram. One point should be pointed that the main frequency is around integral multiple of 3 Hz which is consistent with EEG sequence, since during active seizures high amplitude spikes in the EEG alternate with slow positive waves around 3 Hz.

3.2 Seizure dynamics

Coupling strength between cortex and thalamus cells is found to be crucial for generating different states, so in this section we focus on the seizure pattern. Results demonstrate that periodic patterns that closely resemble the EEG data recorded during human seizure can be carried out through different route. Consistent to experimental finding, seizure patterns can be induced by modulation of varying synaptic transmission as shown in Figure 3.

Figure 3(a) and (b) are presented the seizure initiation through corticothalamic excitation where we linearly increase v_{se} to observe the effects of continuous changes of ϕ_e. There is a gradual increase in the amplitude of ϕ_e presented as abnormal seizure state when v_{se} climbs to reach seizure state, and on ramping down of v_{se}, ϕ_e also declines back to the original normal level.

Similarly, seizure onset by TRN inhibition denoted by v_{sr} can also be found in Figure 3(c) and (d). With the increase of inhibition strength v_{sr} from TRN to SRN, seizure onset activity appears, and then disappears when inhibition strength is set back. Furthermore, it is pointed that the strength of bursting variable g_X and g_H have predominant effect on T-type current which is involved in bursting dynamics of thalamic neurons [45]. Therefore, we study the activities modulated by g_X with the ratio $g_H = 4g_X$ fixed and show the seizure phenomenon due to g_H by upward adjustment of T-current displayed in Figure 3(e) and (f).

The seizure onset by shifting of GABAergic activity towards longer timescale in thalamus appears different that illustrated in Figure 3(g) and (h). We change α with a fixed ratio $= 4\alpha$ to observe the variations of firing ratio ϕ_e, where a lower value of α means a longer timescale.

Besides, it is arguably that there are four classical firing states observed in brain activity as shown in Figure 4. Our modeling can successfully repeat these four state: low firing

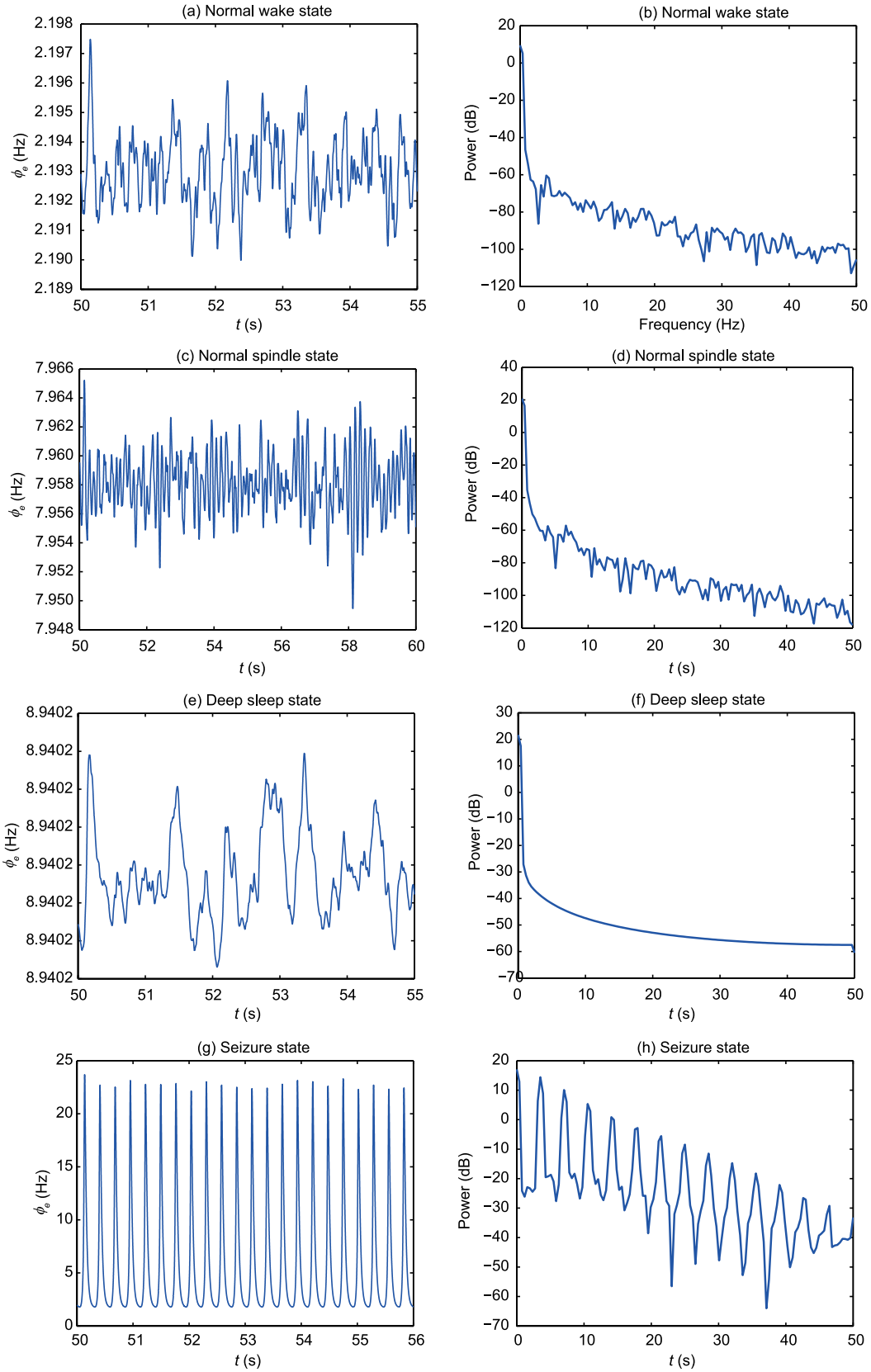

Figure 2 (Color online) Four classical activity states produced by our model. (a) Sequential firing ratio of the normal wake state; (b) frequency spectrum analysis of the normal wake state; (c) sequential firing ratio of the normal spindle state; (d) frequency spectrum analysis of the normal spindle state; (e) sequential firing ratio of the deep sleep; (f) frequency spectrum analysis of the deep sleep state; (g) sequential firing ratio of the seizure state; (h) frequency spectrum analysis of the seizure state. For the convenience of analysis, in the spectrum graphs vertical axis shows the $\log_{10}$ scale of the power spectral density.

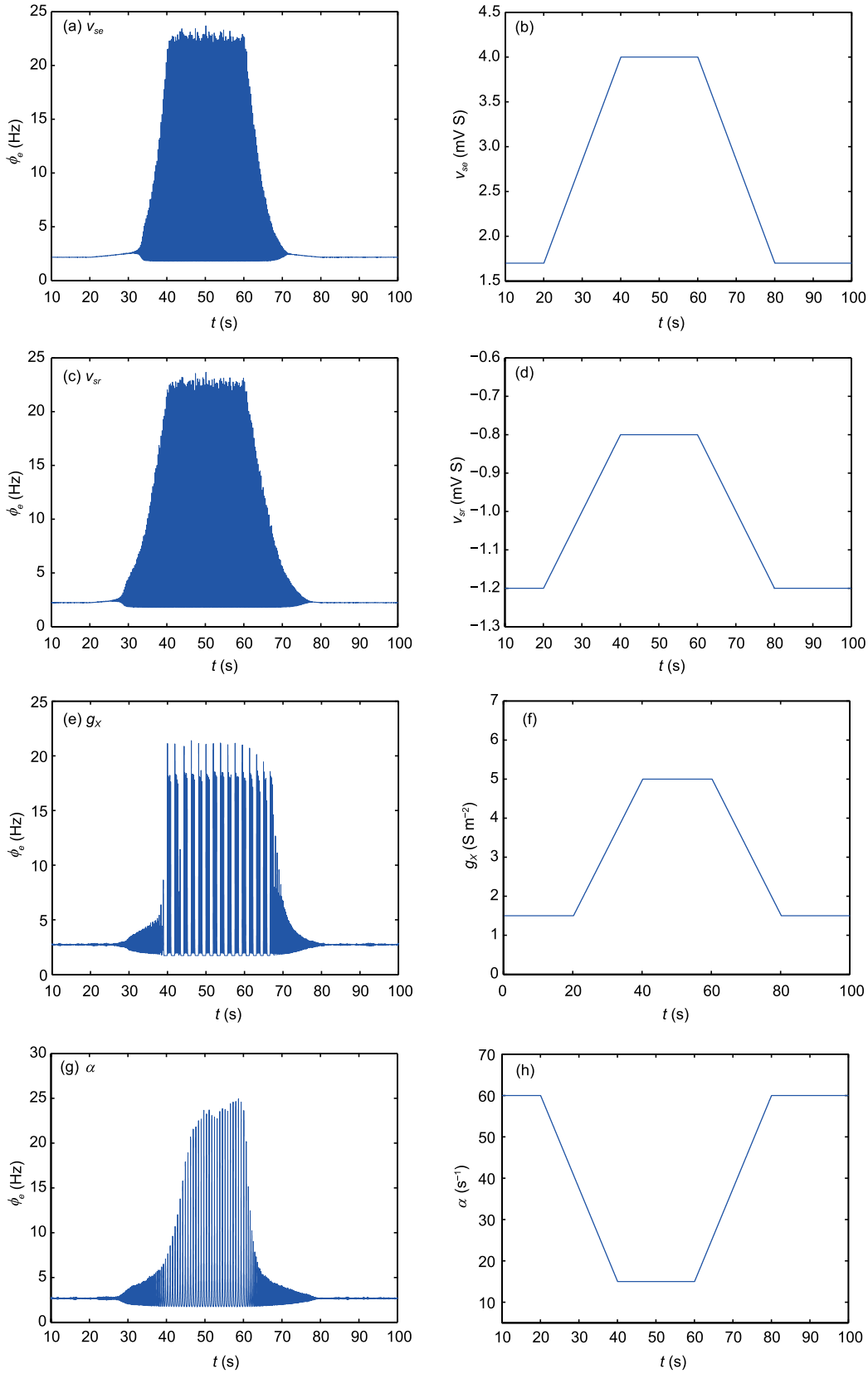

Figure 3 (Color online) Seizure state produced by varying model parameters. (a) Sequential firing ratio arising from increasing excitatory strength v_{se}; (b) time series of parameter v_{se}; (c) sequential firing ratio arising from increasing the inhibitory strength v_{sr}; (d) time series of parameter v_{se}; (e) sequential firing ratio arising from elevating activation of T channels by increasing v_{gX}; (f) time series of parameter g_X; (g) sequential firing ratio arising from decreasing dendritic α; (h) time series of parameter α.

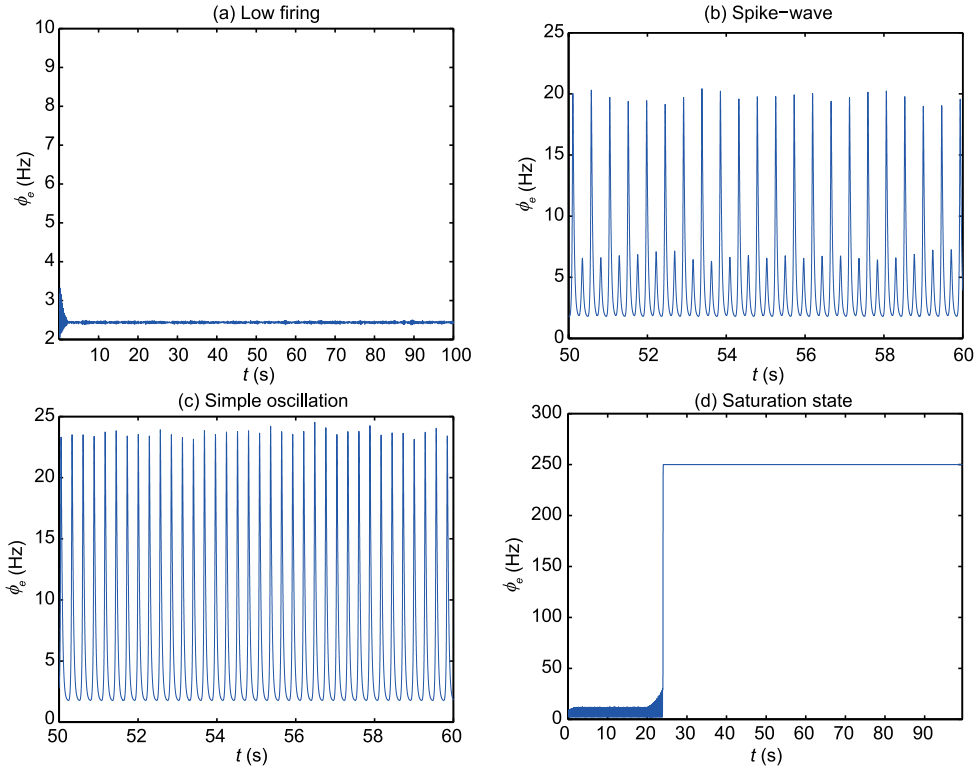

Figure 4 (Color online) Four classical rhythm induced under different set of parameters in our model. (a) Low firing state; (b) spike-wave state; (c) simple oscillation; (d) saturation state.

(Figure 4(a)), spike wave (Figure 4(b)), simple oscillation (Figure 4(c)), and saturation (Figure 4(d)) under different parameter ranges. The phenomenon will be further discussed in the next section.

3.3 Seizure evolution

We first study the effects of v_{se} on the brain activity with the assumption that changes of v_{se} obey linear function. A revolution of rising in the firing ratio can be easily observed from Figure 5(a), (b), (c) and (d). As we escalate v_{se} to high levels, the amplitude of firing ratio in cortex mass increases in size from low firing state (< 5 Hz) which can be classified as normal state, then evolves into the seizure state where the amplitude is above 20 Hz and finally reaches the maximum firing ratio $Q_{\max} = 250$ Hz as the limit set in our model.

Recently, a number of studies on the mean field models have pointed that time delay τ also plays a significant role in the dynamics of spikes. Here the effect of time delay is also studied in abnormal states, which demonstrates that time delay has great effects on the wave forms of ϕ_e. Figure 6 depicts the wave transformation of seizure states as the time delay altering, including simple oscillation to spike wave (Figure 6(a) and (b)) and also to saturation state (Figure 6(c) and (d)).

3.4 State contour

Based on the analysis presented above, we illustrates that the coupling strength v_{se} is a crucial model parameter in the cortex activity. Likewise, data confirms the fact that time delay from RTN to SRN transmission is a key factor mediating the behavior of ϕ_e.

To investigate this further, we employ two parameter continuations to draw a contour plane of v_{se} and τ. This kind of activity maps is an effective method to study the variation of firing activity resulted from two parameters expressed by coordinate axes. Four typical dynamical states are depicted by four colors as explained in the caption of Figure 7, namely, each region within one color can be classified as one from these four states.

It is noted that, along the horizontal coordinate of Figure 7(a), it is confirmed that the coupling strength is in charge of firing rate: from low firing rate to saturation point. However, from the vertical point of view, time delay also affects the wave form in seizure states. Within a certain range of v_{se}, no matter the changes of time delay, it maintains in the same activity status, while what has changed is the wave form of seizure state.

As displayed in Figure 7(b), this kind of phenomenon occurs in the contour graph of inhibitory connection v_{sr} and time delay τ between two GABAergic channels. Comparing Figure 7(a) and (b) have a slight variation on the state sequence, bigger strength of v_{sr} means lower firing state while smaller inhibitory strength leads to saturation.

When considering the effects of both g_X and α with τ, situations become not quite the same as that of synapse strength

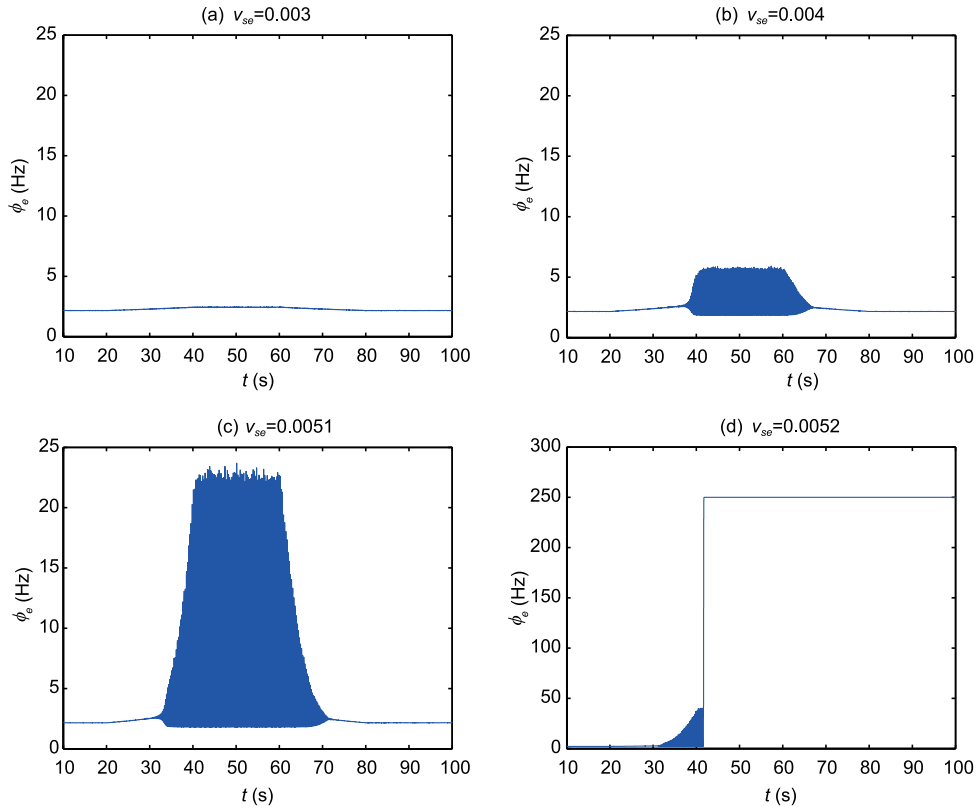

Figure 5 (Color online) Effect of cortico-thalamus excitation on activity states under different v_{se} values, while other model parameters are same fixed. (a) Normal low firing state; (b) pathological state; (c) seizure state; (d) saturation state.

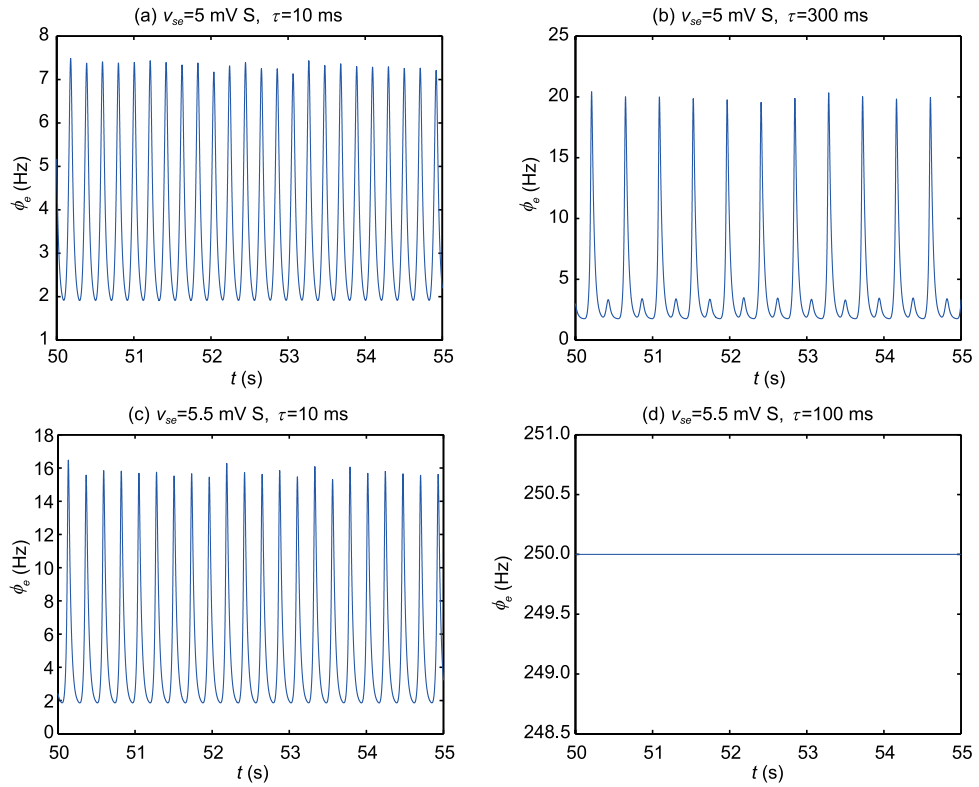

Figure 6 (Color online) Effect of time delay. Different τ under same v_{se} results in different dynamical state. (a) Simple oscillation state; (b) spike-wave state; (c) simple oscillation state; (d) saturation state.

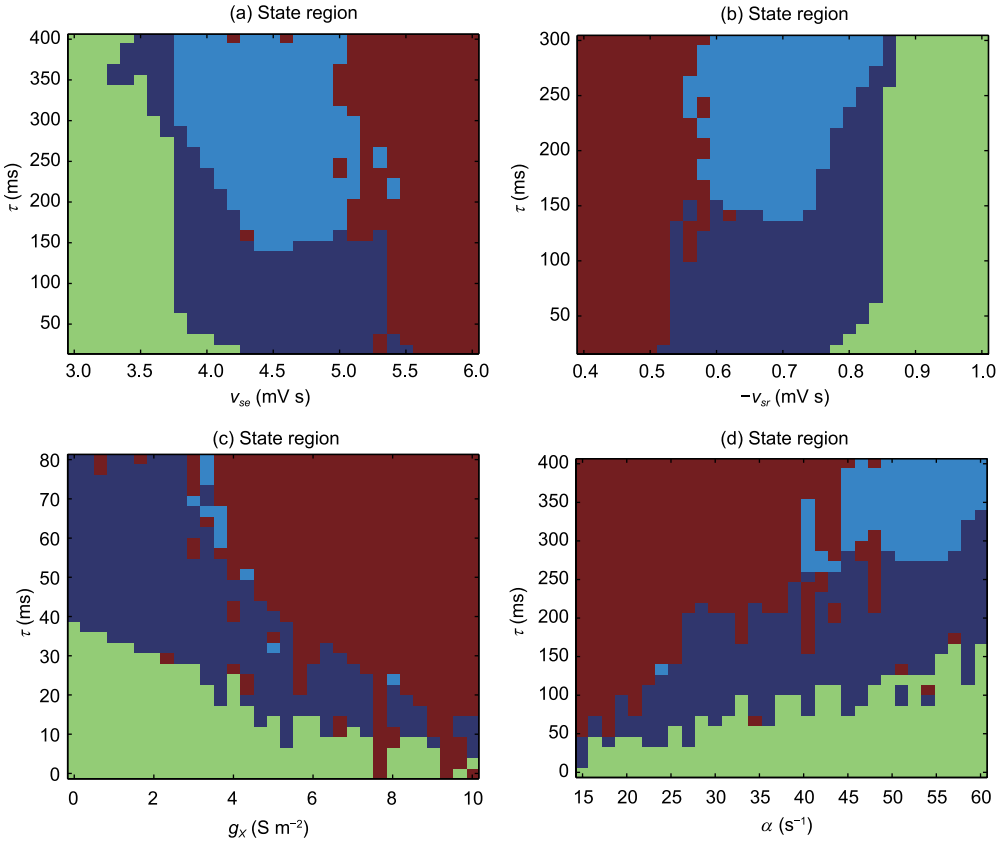

Figure 7 (Color online) Contour graph in two parameter panel. (a) $v_{se}-\tau$; (b) $v_{sr}-\tau$; (c) $g_X-\tau$; (d) $\alpha-\tau$. Region in green color for low firing rate state, red for saturation state, and deep blue for simple oscillation state, light blue for spike-wave state. Dotted regions are not classified due to the margin error.

v_{se} and v_{sr}. The two-dimensional map in (v_{sr}, τ)-space given in Figure 7(c) implies the spike-wave state can hardly exist and will still unlikely arise no matter when either time delay or conductance g_X increases. Situations obtained in the (α, τ) contour get more complex due to the unclear margin caused by simulation error as revealed in Figure 7(d). But it is certain that when time delay is small, firing rate remains low whatever the value of the receptor offset time α and β are.

3.5 Uncertain time-delay

In Figure 7(a), we know that time delay does not affect much on the states if time delay is fixed already, while v_{se} makes a great difference on the states. For a further study, here we propose a random time delay τ instead of fixed time delay which is used in all the above analysis.

Sequence diagraph and spectrogram are plotted in Figure 8 (a)–(h) which demonstrates random time delay has unique effects on activity states. Unlike fixed time delay, time-varying time delay which may vary randomly within a time range can manage seizure state at normal states. Comparing Figure 8(b) and (h), the dominant frequency is gradually down to a normal level lower than 5 Hz as the maximum of time delay increases. In this situation, increasing time delay can suppress the seizure duration.

3.6 Reduced network

Research both in vivo and in vitro experiments has demonstrated that spike wave activity is first initiated SRN and then propagated to the cortex and finally is induced in the TRN [35,36,40,46]. As mentioned in ref. [18], periodic signal can simulate the excitatory drive to the TRN as an approximation to the full mode when seizure state is generated. In this section, we try a reduced model using sinusoidal input to replace the effect of ϕ_e in the completed network.

From Figure 9 we may make a conclusion, this reduced network can emulate the full network model, since spike-wave state and simple oscillation state can be found under some appropriate parameter conditions when studying dynamical behavior of SRN denoted by ϕ_s and TRN denoted by ϕ_r.

4 Conclusion

We have developed a typical and widely used mean-field model to study the clinical EEG data in seizure patients and extensively simulated the dynamical behavior in the cortex-thalamus circuitry. Besides four dynamical states including normal activity and pathological seizure activity were successfully modeled by changing some parameter value in our present model, we mainly studied the generation

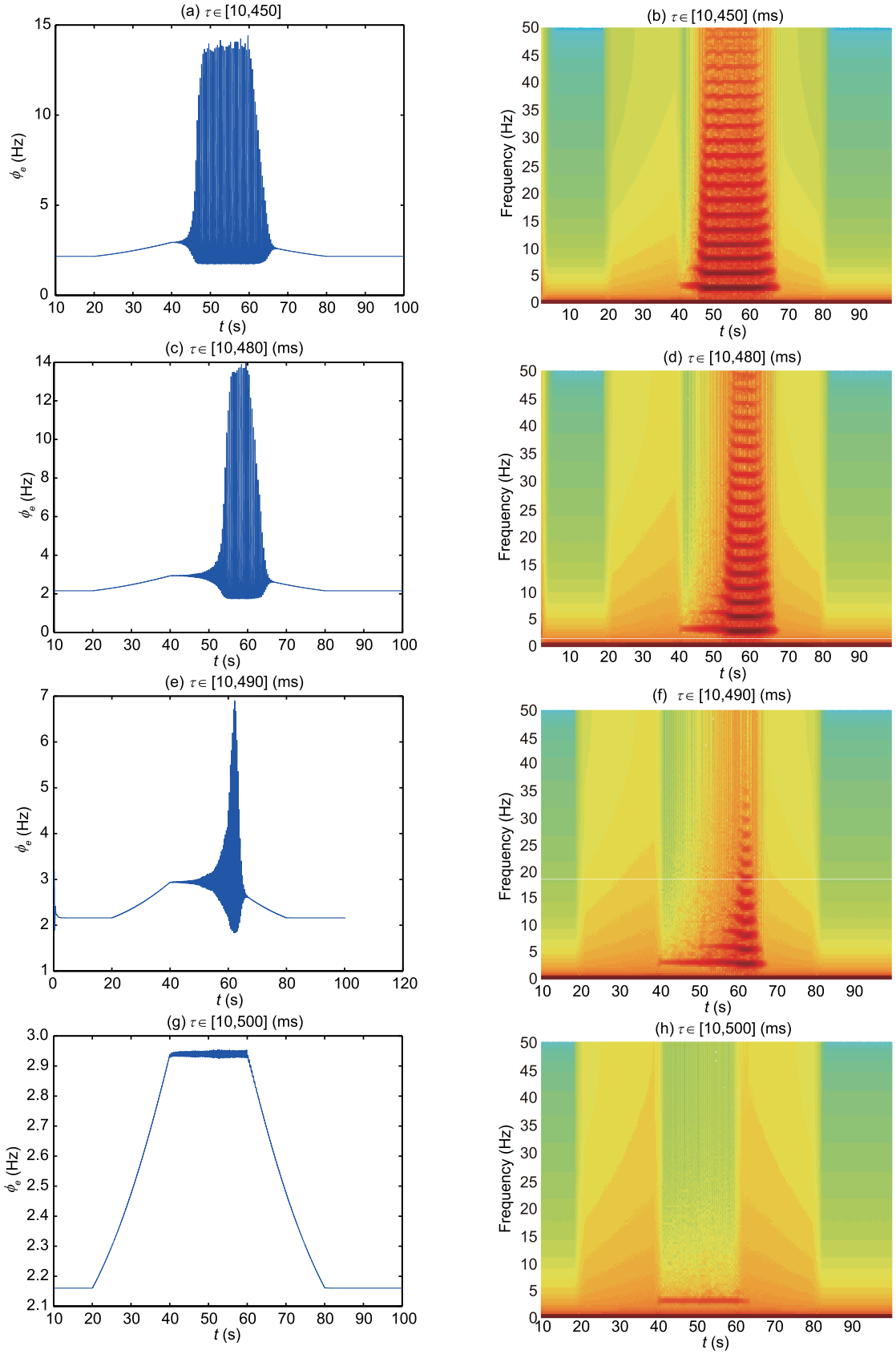

Figure 8 (Color online) Suppression of time-varying delay on dynamical state. (a) Time series of seizure state; (b) spectrogram of seizure state; (c) time series of suppressed seizure duration; (d) spectrogram of suppressed seizure duration; (e) time series of transient attack; (f) spectrogram of transient attack; (g) time series of eliminated seizure; (h) spectrogram of eliminated seizure.

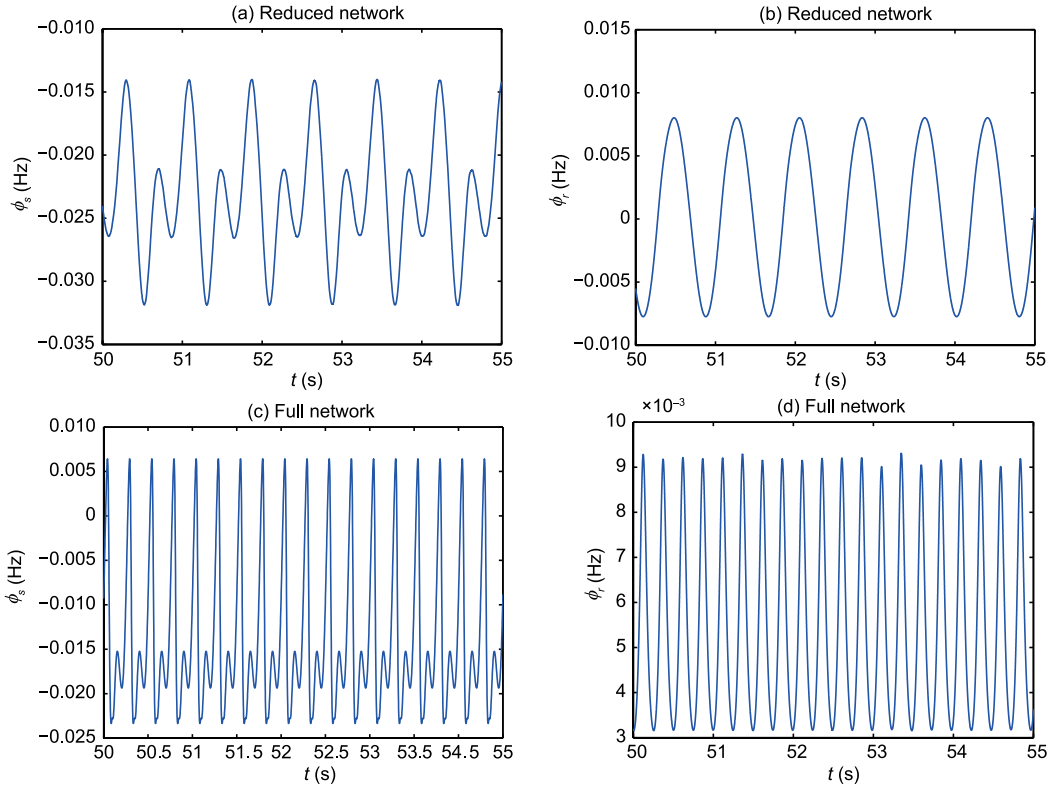

Figure 9 (Color online) Comparison of reduced network and full model. (a) Spike wave form of SRN in simple network; (b) simple oscillation of SRN in simple network; (c) spike wave form of TRN in full network; (d) simple oscillation of TRN in full network.

of seizure state and seizure evolution under different brain connections.

Our results demonstrate that model parameters related to synaptic connection, time delay, conductance, and also slow variable have great effects on the activity state of brain, which implies that multiple pathways can be provided to control and even eliminate seizure spike wave in theoretical model. Based on the simulated results of uncertain time delay illustrated in the Section 3.5, time-varying time delay can also be used to explore for monitoring seizure states. As addition, a reduced work is proved to present the main feature of seizure behavior in general full model, which provides an alternative choose for some situation such as theoretical analysis.

This work was supported by the Foundational Research Funds for the Central Universities (Grant Nos. G2016KY0301) and the National Natural Science Foundation of China (Grant Nos. 11602192 & 11672074).

1 Hauser W A. Epilepsy: A Comprehensive Textbook. Philadelphia: Lippincott- Raven Publishers, 1998
2 Browne T R, Holmes G L. Handbook of Epilepsy. Philadelphia: Williams and Wilkins, 2000
3 Aarabi A, He B. Seizure prediction in hippocampal and neocortical epilepsy using a model-based approach. Clin Neurophysiol, 2014, 125: 930–940
4 Ullah G, Schiff S J. Assimilating seizure dynamics. PLoS Comput Biol, 2010, 6: e1000776
5 Stefanescu R A, Shivakeshavan R G, Talathi S S. Computational models of epilepsy. Seizure, 2012, 21: 748–759
6 Silva F L, Blanes W, Kalitzin S N, et al. Epilepsies as dynamical diseases of brain systems: Basic models of the transition between normal and epileptic activity. Epilepsia, 2003, 4: 72–83
7 Milton J G. Epilepsy as a dynamic disease: A tutorial of the past with an eye to the future. Epilepsy Behav, 2010, 18: 33–44
8 Taylor P N, Goodfellow M, Wang Y, et al. Towards a large-scale model of patient-specific epileptic spike-wave discharges. Biol Cybern, 2013, 107: 83–94
9 Taylor P N, Kaiser M, Dauwels J. Structural connectivity based whole brain modelling in epilepsy. J Neurosci Meth, 2014, 236: 51–57
10 Yan B, Li P. The emergence of abnormal hypersynchronization in the anatomical structural network of human brain. NeuroImage, 2013, 65: 34–51
11 Baier G, Goodfellow M, Taylor P N, et al. The importance of modeling epileptic seizure dynamics as spatio-temporal patterns. Front Physiol, 2012, 3: 00281
12 Saillet S, Gharbi S, Charvet G, et al. Neural adaptation to responsive stimulation: A comparison of auditory and deep brain stimulation in a rat model of absence epilepsy. Brain Stimulation, 2013, 6: 241–247
13 Conte A, Gilio F, Iacovelli E, et al. Effects of repetitive transcranial magnetic stimulation on spike-and-wave discharges. Neurosci Res, 2007, 57: 140–142
14 Freeman W J. Mass Action in The Nervous System. New York: Academic Press, 1975
15 Wilson H R, Cowan J D. A mathematical theory of the functional dynamics of cortical and thalamic nervous tissue. Kybernetik, 1973, 13: 55–80
16 Wendling F, Bartolomei F, Bellanger J J, et al. Epileptic fast activity can be explained by a model of impaired GABAergic dendritic inhibition. Eur J Neurosci, 2002, 15: 1499–1508

17 Jansen B H, Rit V G. Electroencephalogram and visual evoked potential generation in a mathematical model of coupled cortical columns. Biol Cybern, 1995, 73: 357–366
18 Jansen B H, Zouridakis G, Brandt M E. A neurophysiologically-based mathematical model of flash visual evoked potentials. Biol Cybern, 1993, 68: 275–283
19 Zandt B J, Visser S, van Putten M J A M, et al. A neural mass model based on single cell dynamics to model pathophysiology. J Comput Neurosci, 2014, 37: 549–568
20 de Haan W, Mott K, van Straaten E C W, et al. Activity dependent degeneration explains hub vulnerability in alzheimer's disease. PLoS Comput Biol, 2012, 8: e1002582
21 Pons A J, Cantero J L, Atienza M, et al. Relating structural and functional anomalous connectivity in the aging brain via neural mass modeling. Neuroimage, 2010, 52: 848–861
22 Deco G, Jirsa V K, Robinson P A, et al. The dynamic brain: From spiking neurons to neural masses and cortical fields. PLoS Comput Biol, 2008, 4: e1000092
23 Taylor P N, Baier G. A spatially extended model for macroscopic spike-wave discharges. J Comput Neurosci, 2011, 31: 679–684
24 Taylor P N, Wang Y, Goodfellow M, et al. A computational study of stimulus driven epileptic seizure abatement. PLoS One, 2014, 9: e114316
25 Velazquez J L P, Huo J Z, Dominguez L G, et al. Typical versus atypical absence seizures: Network mechanisms of the spread of paroxysms. Epilepsia, 2007, 48: 1585–1593
26 Dulac O. Epileptic encephalopathy. Epilepsia, 2001, 42: 23–26
27 Loddenkemper T, Fernández I S, Peters J M. Continuous spike and waves during sleep and electrical status epilepticus in sleep. J Clin Neurophysiol, 2011, 28: 154–164
28 Robinson P A, Rennie C J, Rowe D L. Dynamics of large-scale brain activity in normal arousal states and epileptic seizures. Phys Rev E, 2002, 65: 041924
29 Breakspear M, Roberts J A, Terry J R, et al. A unifying explanation of primary generalized seizures through nonlinear brain modeling and bifurcation analysis. Cereb Cortex, 2005, 16: 1296–1313
30 Suffczynski P, Kalitzin S, Lopes Da Silva F H. Dynamics of non-convulsive epileptic phenomena modeled by a bistable neuronal network. Neuroscience, 2004, 126: 467–484
31 Kim J W, Robinson P A. Compact dynamical model of brain activity. Phys Rev E, 2007, 75: 031907
32 Robinson P A, Wu H, Kim J W. Neural rate equations for bursting dynamics derived from conductance-based equations. J Theor Biol, 2008, 250: 663–672
33 Marten F, Rodrigues S, Benjamin O, et al. Onset of polyspike complexes in a mean-field model of human electroencephalography and its application to absence epilepsy. Philos Trans R Soc A-Math Phys Eng Sci, 2009, 367: 1145–1161
34 Kim J W, Robinson P A. Controlling limit-cycle behaviors of brain activity. Phys Rev E, 2008, 77: 051914
35 Ursino M, Cona F, Zavaglia M. The generation of rhythms within a cortical region: Analysis of a neural mass model. Neuroimage, 2010, 52: 1080–1094
36 Robinson P A, Rennie C J, Wright J J. Propagation and stability of waves of electrical activity in the cerebral cortex. Phys Rev E, 1997, 56: 826–840
37 Destexhe A. Spike-and-wave oscillations based on the properties of GABA(B) receptors. J Neurosci, 1998, 18: 9099–9111
38 Destexhe A, Huguenard J R. Nonlinear thermodynamic models of voltage dependent currents. J Comp Neurosci, 2000, 9: 259–270
39 Nunez P L, Srinivasan R. Electric Fields of the Brain: The Neurophysics of EEG. Oxford: Oxford University Press, 2006
40 Jirsa V K, Haken H. Field theory of electromagnetic brain activity. Phys Rev Lett, 1996, 77: 960–963
41 Marten F, Rodrigues S, Suffczynski P, et al. Derivation and analysis of an ordinary differential equation mean-field model for studying clinically recorded epilepsy dynamics. Phys Rev E, 2009, 79: 021911
42 Wilson H R, Cowan J D. Excitatory and inhibitory interactions in localized populations of model neurons. Biophys J, 1972, 12: 1–24
43 Rodrigues S, Terry J R, Breakspear M. On the genesis of spike-wave oscillations in a mean-field model of human thalamic and corticothalamic dynamics. Phys Lett A, 2006, 355: 352–357
44 Zhao X, Robinson P A. Generalized seizures in a neural field model with bursting dynamics. J Comput Neurosci, 2015, 39: 197–216
45 Bazhenov M, Timofeev I, Steriade M, et al. Model of thalamocortical slow-wave sleep oscillations and transitions to activated states. J Neurosci, 2002, 22: 8691–8704
46 Destexhe A, Sejnowski T J. Interactions between membrane conductances underlying thalamocortical slow-wave oscillations. Physiol Rev, 2003, 83: 1401–1453